Sciences & Technologie **A** – **N°30** Décembre. (2009), pp. 23-30

Numerical approach of the natural convection in the annular space delimited by two horizontal eccentric cylinders: relative eccentricity effect

Reçu le 04/12/2008 – Accepté le 13/010/2009

C. GHERNOUG
M. DJEZZAR

Department of Physics
Energetic Physics Laboratory
University Mentouri Constantine
Algeria

Résumé

Mots clés:

Abstract

The authors propose in this work, the numerical study of the phenomenon of the natural laminar permanent convection in an annular space, situated between two horizontal eccentric cylinders and tilted of an angle α compared to the horizontal one. The enclosure considered is of practical interest (Storage, Isolation). The annular space is filled by a Newtonian and incompressible fluid. The number of Prandtl is fixed at 0.7 (case of the air) but the number of Grashof varies. By using the approximation of Boussinesq and the vorticity-stream function formulation, the flow is modeled by the differential equations with the derivative partial: the equations of continuity and the momentum are expressed in a frame of reference known as "bicylindrical", to facilitate the writing of the boundary conditions and to transform the curvilinear field into a rectangular one. They examine the effect of the Grashof number, the parietal thermal conditions and tilt of the system.

Keywords: natural convection/ annular space/bicylindrical coordinates/ vorticity-stream function formulation

ملخص

الكلمات المفتاحيـــة :

Nomenclature

a	Constant seen in the eccentric coordinates	(m)
C_1	Radius ratio	
C_2	Eccentricity of the annular space formed by two eccentric cylinders	
c_p	Specific heat at constant pressure	($j.kg^{-1}.k^{-1}$)
g	Gravitational acceleration	($m.s^{-2}$)
Gr	Grashof number defined by $Gr = \frac{g\beta a^3}{\upsilon^2}\Delta T$	
h	Dimensional metric coefficient	(m)
H	Dimensionless metric coefficient	
Nu	Local Nusselt number	
$\overline{Nu}$	Average Nusselt number	
Pr	Prandtl number defined by $Pr = \frac{\nu \rho c_p}{\lambda}$	
q	Heat flux density	($W.m^{-2}$)
r_1, r_2	Inner and outer radius respectively	(m)
S_Φ	Source term	
T	Fluid's temperature	(K)
T_1	Hot wall temperature	(K)
T_2	Cold wall temperature	(K)
ΔT	Temperature deference $\Delta T=T_1-T_2$	(K)
V_η, V_θ	Velocity components η et θ	($m.s^{-1}$)
$\boldsymbol{V}$	Velocity vector	($m.s^{-1}$)

Greek letters

α	Angle of inclination	(°)
β	Thermal expansion coefficient	(K^{-1})
Γ_φ	Diffusion Coefficient	
λ	Thermal conductivity	($W.m^{-1}.K^{-1}$)
υ	Kinematic viscosity	($m^2.s^{-1}$)
ρ	Fluid density	($kg.m^{-3}$)
η, θ, z	bicylindrical coordinates	
Ψ	Stream function	($m^2.s^{-1}$)
ω	Vorticity	(s^{-1})
φ	General function	
Π	Stress tensor	

Superscripts

+	Dimensionless parameter

Subscripts

i	Inner
e	Outer
Ni	Points number along the coordinate η
NN	Points number along the coordinate θ

1. Introduction

Heat transfer by natural convection, in the annular spaces formed by horizontal eccentric cylinders, was the subject of many theoretical and experimental studies because of their importance in many engineering applications.

Nobari et al [1] studied numerically the fluid flow and heat transfer in curved eccentric annuli. A second order finite difference method based on the Projection algorithm is implemented to solve the governing equations including the full Navier–Stokes, the continuity, and the energy equations in a toroïdal coordinate system.

It is also shown that in contrast to straight eccentric annuli, heat transfer rates can be augmented in the eccentric curved annuli comparing with the straight concentric annuli at the large dean numbers. Shklyar et al [2] analyzed the convergence rate of a methodology for solving incompressible flow in general curvilinear co-ordinates. Overset grids (double-staggered grids type), each defined by the same boundaries as the physical domain are used for discretization. Dukaa et al [3] proposed two different problems as approximations of the usual system modelling natural convection under the Oberbeck–Boussinesq assumptions. The average Nusselt number is also estimated. Shi et al [4] applied this model to simulate natural convection heat transfer in a horizontal concentric annulus bounded by two stationary cylinders with different temperatures. Velocity and temperature distributions as well as Nusselt numbers were obtained for the Rayleigh numbers ranging from $2.38x10^3$ to 1.02×10^5 with the Prandtl number around 0.718.

Roschina et al [5] investigated Natural convection of gas (Pr = 0.7) between two horizontal coaxial cylinders with uniform internal heat generation. It has been established that in such a system there exist two types of fluid flow for low Rayleigh numbers with different vortex structure. Optimization of the corresponding coaxial laser system has been analyzed.

In this work we have numerical simulation which uses finite volumes method, exposed by Patankar [6], bicylindrical coordinates cited by Moon [7] and vorticité-stream function formulation cited by Nogotov [8] to solve the equations.

2. Problem formulation and basic equations

Let's consider an annular space, filled with an incompressible Newtonian fluid, situated between two eccentric cylinders. Figure 1 represents a cross-section of the system.

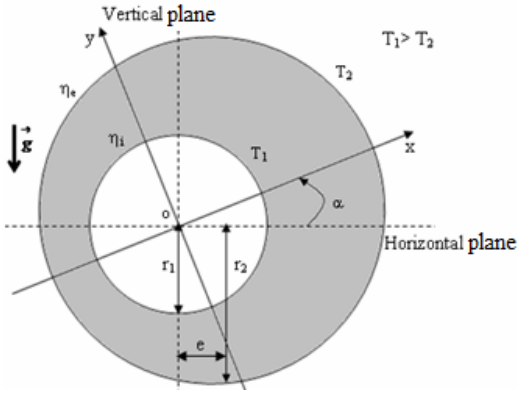

Fig. 1 a cross-section of the system

The inner and outer cylindric walls are isotherms which are held at temperatures T_1 and T_2 with $T_1>T_2$, in a first case of heating, in a second case of heating, we impose on the inner cylinder a constant heat flux density. The

physical properties of the fluid are constant, except the density ρ whose variations are at the origin of the natural convection. Viscous dissipation is neglected, just as the radiation (emissive properties of the two walls being neglected). We admit that the problem is bidimensionnal, permanent and laminar.

- Continuity equation:

$$\mathbf{div}\, \mathbf{V} = 0 \quad (1)$$

Momentum equation:

$$(\boldsymbol{V}.\mathbf{grad})\boldsymbol{V} = \frac{\rho}{\rho_0}\boldsymbol{g} + \frac{\Delta\Pi}{\rho_0} \quad (2)$$

- Heat equation:

$$(\boldsymbol{V}.\mathbf{grad})T = \frac{\lambda}{\rho c_p}\nabla^2 T \quad (3)$$

The coordinates are:

$$\left.\begin{aligned} x &= \frac{a\,sh(\eta)}{ch(\eta)-\cos(\theta)} \\ y &= \frac{a\,sin(\eta)}{ch(\eta)-\cos(\theta)} \\ z &= z \end{aligned}\right\} \quad (4)$$

The equations (1), (2) and (3) become:

$$\frac{\partial}{\partial\eta}\left(hV_\eta\right) + \frac{\partial}{\partial\theta}\left(hV_\theta\right) = 0 \quad (5)$$

$$\frac{V_\eta}{h}\frac{\partial\omega}{\partial\eta} + \frac{V_\theta}{h}\frac{\partial\omega}{\partial\theta} = \frac{g\beta}{h}\left\{\begin{aligned}&[F(\eta,\theta)\cos(\alpha) + G(\eta,\theta)\sin(\alpha)]\frac{\partial T}{\partial\eta}\\ &+[F(\eta,\theta)\sin(\alpha) - G(\eta,\theta)\cos(\alpha)]\frac{\partial T}{\partial\theta}\end{aligned}\right\} + \frac{\upsilon}{h^2}\left(\frac{\partial^2\omega}{\partial\eta^2} + \frac{\partial^2\omega}{\partial\theta^2}\right) \quad (6)$$

$$V_\eta\frac{\partial T}{\partial\eta} + V_\theta\frac{\partial T}{\partial\theta} = \frac{\lambda}{\rho cp}\frac{1}{h}\left(\frac{\partial^2 T}{\partial\eta^2} + \frac{\partial^2 T}{\partial\theta^2}\right) \quad (7)$$

After the introduction of vorticity defined by:

$$\omega = -\frac{1}{h^2}\left(\frac{\partial^2\psi}{\partial\eta^2} + \frac{\partial^2\psi}{\partial\theta^2}\right) \quad (8)$$

$$\left.\begin{aligned} h &= \frac{a}{(ch(\eta)-\cos(\theta))} \\ F(\eta,\theta) &= \frac{1-ch(\eta)\cos(\theta)}{(ch(\eta)-\cos(\theta))} \\ G(\eta,\theta) &= \frac{sh(\eta)\sin(\theta)}{(ch(\eta)-\cos(\theta))} \end{aligned}\right\} \quad (9)$$

We pass directly to the writing dimensionless equations, by posing the following dimensionless quantities:

$D_h = a$

$$H = \frac{h}{D_h},\ V_\eta^+ = V_\eta\frac{D_h}{\upsilon},\ V_\theta^+ = V_\theta\frac{D_h}{\upsilon},\ \omega^+ = \omega\frac{D_h^2}{\upsilon},$$

$$\psi^+ = \frac{\psi}{\upsilon} \text{ and } T^+ = \frac{T-T_2}{T_1-T_2}$$

The equations (5), (6), (7) and (8) become :

$$V_\eta\frac{\partial}{\partial\eta}\left(HV_\eta^+\right) + V_\theta\frac{\partial}{\partial\theta}\left(HV_\theta^+\right) = 0 \quad (10)$$

$$\frac{V_\eta^+}{H}\frac{\partial\omega^+}{\partial\eta} + \frac{V_\theta^+}{H}\frac{\partial\omega^+}{\partial\theta} = \frac{Gr}{H}\left\{\begin{aligned}&[F(\eta,\theta)\cos(\alpha) + G(\eta,\theta)\sin(\alpha)]\frac{\partial T^+}{\partial\eta}\\ &+[F(\eta,\theta)\sin(\alpha) - G(\eta,\theta)\cos(\alpha)]\frac{\partial T^+}{\partial\theta}\end{aligned}\right\} + \frac{1}{H^2}\left(\frac{\partial^2\omega^+}{\partial\eta^2} + \frac{\partial^2\omega^+}{\partial\theta^2}\right) \quad (11)$$

$$HV_\eta^+\frac{\partial T^+}{\partial\eta} + HV_\theta^+\frac{\partial T^+}{\partial\theta} = \frac{1}{Pr}\left(\frac{\partial^2 T^+}{\partial\eta^2} + \frac{\partial^2 T^+}{\partial\theta^2}\right) \quad (12)$$

$$\omega^+ = -\frac{1}{H^2}\left(\frac{\partial^2\psi^+}{\partial\eta^2} + \frac{\partial^2\psi^+}{\partial\theta^2}\right) \quad (13)$$

The boundary conditions are the following ones:

- Inner cylinder wall Condition (η=ηi=constant):

$$V_\eta^+ = V_\theta^+ = \frac{\partial\psi^+}{\partial\eta} = \frac{\partial\psi^+}{\partial\theta} = 0,$$

$$\omega^+ = -\frac{1}{H^2}\left(\frac{\partial^2\psi^+}{\partial\eta^2} + \frac{\partial^2\psi^+}{\partial\theta^2}\right) \text{ and}$$

$$q_{constant} = \lambda\frac{1}{h}\frac{\partial T}{\partial\eta}\Big|_{\eta=\eta_i}$$

- **Case I :** $T_1^+ = 1$
- **Case II :** $\frac{1}{H}\frac{\partial T^+}{\partial\eta}\Big|_{\eta=\eta_i} = -1$

- Outer cylinder wall Condition ($\eta=\eta_e$=constant):

$$V_\eta^+ = V_\theta^+ = \frac{\partial\psi^+}{\partial\eta} = \frac{\partial\psi^+}{\partial\theta} = 0,$$

$$\omega^+ = -\frac{1}{H^2}\left(\frac{\partial^2\psi^+}{\partial\eta^2} + \frac{\partial^2\psi^+}{\partial\theta^2}\right) \text{ and } T_2^+ = 0$$

The temperatures distribution obtained local Nusselt number value relation:

$$Nu = -\frac{1}{H}\frac{\partial T^+}{\partial\eta}\Big|_{\eta=cste} \quad (14)$$

The average Nusselt number is:

$$\overline{Nu} = \frac{1}{\theta_{NN}-\theta_1}\int_{\theta_1}^{\theta_{NN}} Nu\,d\theta \quad (15)$$

3. Numerical Formulation

To solve the equations (11) and (12) with the associated boundary conditions, we consider a numerical solution by the method of finite volumes, exposed by Patankar [6]. For the equation (13), we consider a numerical solution by the method of the centered differences, exposed by Nogotov [8].

	Γ_φ	S_φ
T^+	$1/Pr$	0
ω^+	1	$HGr\left\{\begin{matrix}[F(\eta,\theta)\cos(\alpha)+G(\eta,\theta)\sin(\alpha)]\frac{\partial T^+}{\partial \eta} \\ +[F(\eta,\theta)\sin(\alpha)-G(\eta,\theta)\cos(\alpha)]\frac{\partial T^+}{\partial \theta}\end{matrix}\right\}$

Figure 2 represents physical and computational domain.

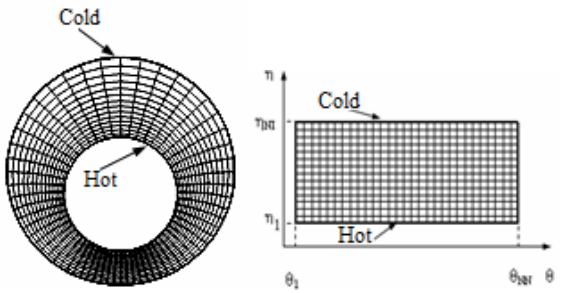

Physical Domain computational domain

Fig. 2 physical and computational domain

We cut out the enclosure according to directions x and y from the whole of elementary volumes or "control volumes" equal to «Δx.Δy.1». ». The problem is two-dimensional, the thickness in z direction is assumed to the unity.

The center of a typical control volume is a point P and the center of its side faces "east", "west", "north" and "south", are the points e, w, n and s, respectively. Four other control volumes surround each interior control volume. The centers of these volumes are points E, W, N and S.

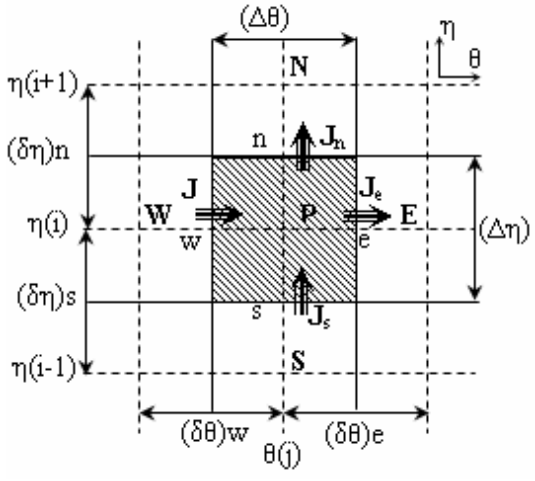

Fig. 3 A typical control volume and its neighbors in a computational domain

3.1. Discretization equation transfer of a variable φ

The general differential equation is:

$$\frac{\partial}{\partial \eta}\left(HV_\eta^+\varphi-\Gamma_\varphi\frac{\partial \varphi}{\partial \eta}\right)+\frac{\partial}{\partial \theta}\left(HV_\theta^+\varphi-\Gamma_\varphi\frac{\partial \varphi}{\partial \theta}\right)=S_\varphi \quad (16)$$

We illustrate sources and diffusion coefficients in table 1

Table 1: Sources and diffusion coefficients

The discretization equation is obtained by integrating the conservation equation over the control volume shown in figure 3, after some manipulations we have the final discretization equation:

$$a_P\varphi_P = a_N\varphi_N + a_S\varphi_S + a_E\varphi_E + a_W\varphi_W + b \quad (17)$$

The equation coefficients are well defined in Patankar [6]. The power law scheme is used to discretize the convective terms in the governing equations.

4. Results and discussion

We consider three annular spaces formed by eccentric cylinders with three values of inclination angle (α=0°, 45° and 90°) and relative eccentricity (C_2=0.4).

4.1. Grid study

In this study several grids were used arbitrarily, to see their effect on the results. Table 2 shows us the variation of average Nusselt number and the maximum of the stream function value according to the number of nodes for each grid. We choose the grid (101x111).

	Gr=10^3		Gr=5.10^4		Gr=10^5		Gr=10^6	
nixnn	ψ_{max}	|Er| %	ψ_{max}	|Er| %	ψ_{max}	|Er| %	ψ_{max}	|Er| %
21x31	1.32	-	5.23	-	8.86	-	34.99	-
31x41	1.34	1.49	5.28	0.94	9.04	1.99	34.41	1.65
41x41	1.34	0.00	5.29	0.19	8.93	1.21	33.99	1.65
51x61	1.33	0.75	5.26	0.57	8.81	1.34	33.58	1.17
61x71	1.31	1.50	5.20	1.14	8.72	1.02	33.29	0.83
71x81	1.29	1.52	5.15	0.96	8.64	0.91	33.06	0.67
81x91	1.28	0.77	5.09	1.16	8.56	0.92	32.85	0.63
91x101	1.27	0.78	5.04	0.98	8.46	1.16	32.64	0.63
101x111	1.25	1.57	4.98	1.19	8.37	1.06	32.45	0.58
111x121	1.24	0.80	4.93	1.00	8.30	0.83	32.29	0.49

Table 2 variation of average Nusselt number and the maximum of the stream function value according to the number of nodes

4.2. Numerical code validation

Kuehn et al. [9] developed a numerical study on natural convection in the annulus between two concentric cylinders and horizontal with a radius ratio was taken equal to 2.6, they calculated a local equivalent thermal conductivity, defined as the ratio of a temperature gradient in a convective heat exchange on a temperature gradient in a conduction exchange:

$$\lambda_{eq} = \frac{\left.\frac{\partial T^+}{\partial \eta}\right|_{convection}}{\left.\frac{\partial T^+}{\partial \eta}\right|_{conduction}}$$

They calculated an average value of the conductivity.

We applied our computer code to this case and we compared the average Nusselt number value of our results with theirs, we notice that they are in concord. Table 3 illustrates this comparison well.

Numerical study	Pr	0,70	0,70	0,70	0,70
	Ra	10^2	10^3	$6x10^3$	10^4
Inner wall	Kuehn [9]	1,000	1,081	1,736	2,010
	our calculs	1,000	1,066	1,730	2,068
	|E (%)|	**0,000**	**1,388**	**0,346**	**2,886**
Outer wall	Kuehn [9]	1,002	1,084	1,735	2,005
	our calculs	1,002	1,066	1,736	2,078
	|E (%)|	**0,000**	**1,661**	**0,058**	**3,641**

Table 3 Comparison of the average thermal conductivity of Kuehn [9] with our results

4.3. First condition of heating: isotherm inner cylinder

4.3.1.Influence of the Grashof number

4.3.1.1. Isotherms and streamlines

Figures 4 and 5 represent the isotherms and the streamlines for different values of the Grashof number when the relative eccentricity C_2=0.4 and α=90°.

These figures show that the structure of the flow is bicellular. The flow turns in the trigonometrically direction in the left side and in the opposite direction in the right one.

When the Grashof number is equal to 10^4, the heat transfer is essentially conductive, so the isotherms of figure 3 are almost parallel to the walls. Nevertheless there is a movement of the fluid: the particles, which warm up on the hot wall, tend to rise along this one, then to go down again along the cold wall. Thus the flow is organized in two principal cells which turn very slowly in opposite directions.

For $Gr=5.10^4$ the isotherms change appreciably to follow the direction of the flow, and the values of the streamlines mentioned on the same figure increase also appreciably, which translates a transformation of the conductive transfer to the convective transfer.

However, for $Gr=10^6$ the isothermal lines are modified and eventually take the form of a mushroom. The temperature distribution is decreasing in the hot wall towards the cold wall. The direction of the deformation of the isotherms is consistent with the direction of rotation of the streamlines. In laminar flow, we can say that under the action of the movement of particles flying from the hot wall at the symmetry axis, the isothermal lines are away from the wall there. The values of the stream function increase which means that convection increases.

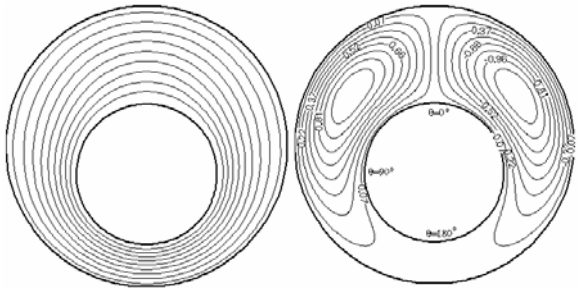

Fig. 4 Isotherms and streamlines for C2=0.4, α=90° and $Gr=10^4$

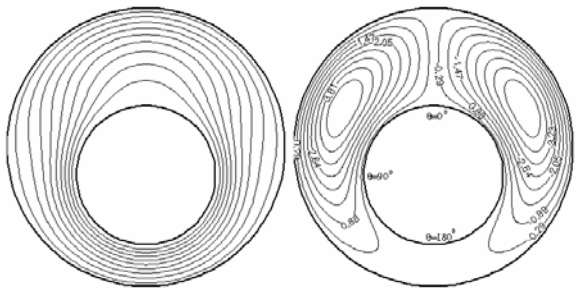

Fig. 5 Isotherms and streamlines for C_2=0.4, α=90° and $Gr=5.10^4$

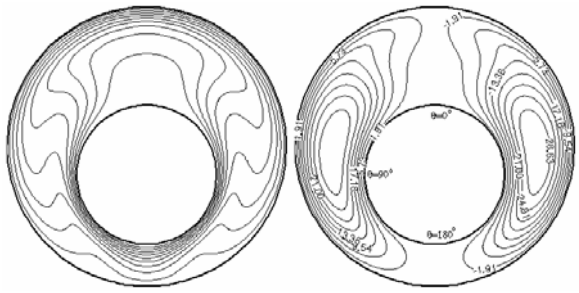

Fig. 6 Isotherms and streamlines for C2=0.4, α=90° and $Gr=10^6$

4.3.2.Local Nusselt Number

We determine the local Nusselt numbers for which changes along the walls are closely related to distributions of isotherms and isocourants, so that, qualitatively, these variations and distributions can often be deduced from each other. For example, if we consider a current point on a wall following a coordinated observation of a monotonic decrease local Nusselt number corresponds to a flow directed along this coordinate, the observation of an increase corresponds to a directed flow in opposite directions.

4.3.3. Variation of local Nusselt number on the inside and outside wall

Figures (7-12) illustrate the variation of local Nusselt number on the inner and outer cylinder wall. We note that with the increase of Grashof number, the value of the local Nusselt number increases and with the decrease of Grashof number, the local Nusselt number decreases.

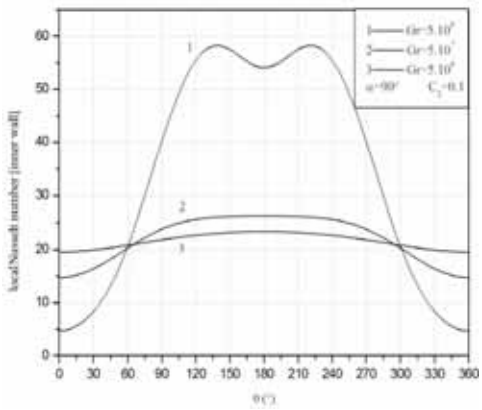

Fig. 7 Variation of local Nusselt number in the inner wall

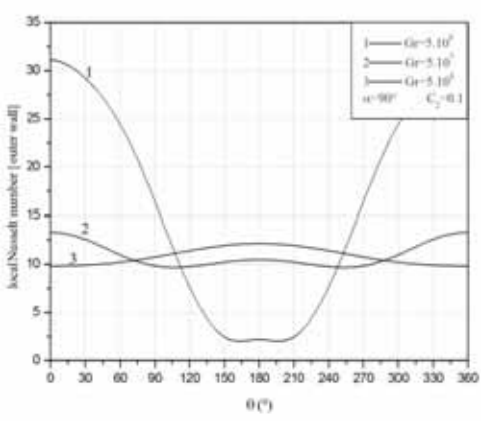

Fig. 8 Variation of local Nusselt number in the outer wall

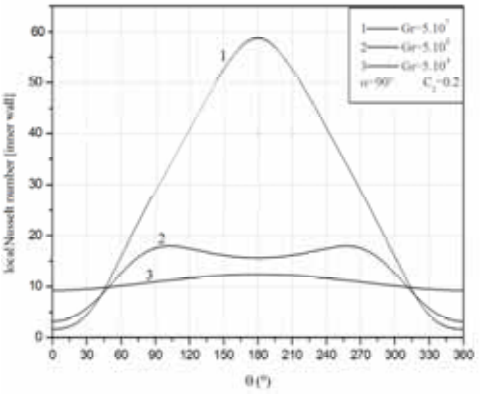

Fig. 9 Variation of local Nusselt number in the inner wall

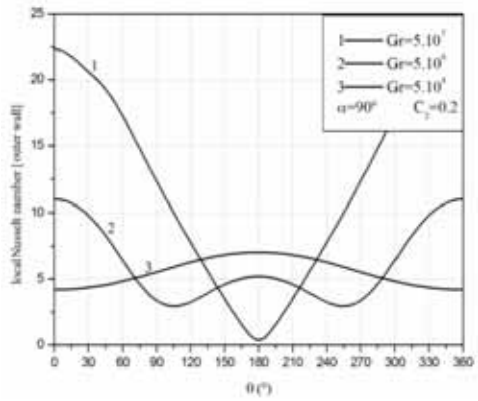

Fig. 10 Variation of local Nusselt number in the outer wall

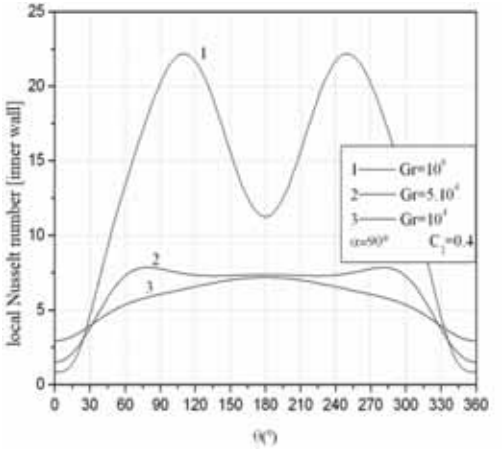

Fig. 11 Variation of local Nusselt number in the inner wall

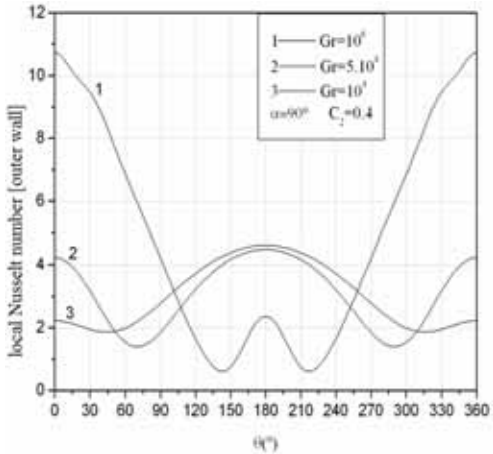

Fig. 12 Variation of local Nusselt number in the outer wall

4.4. Relative eccentricity effect

Here we examine the effect of the relative eccentricity C_2. For the value of the inclination angle α=90 °, we used three values of C_2 (0.1, 0.2 and 0.4).

4.4.1.If the relative eccentricity C_2 = 0.1

Figure 13 shows that the isotherms are parallel to the walls, and the streamlines are symmetrical compared to the median fictitious vertical plane. The Stream function values are very low, this expresses that is the pseudo-conduction which dominates.

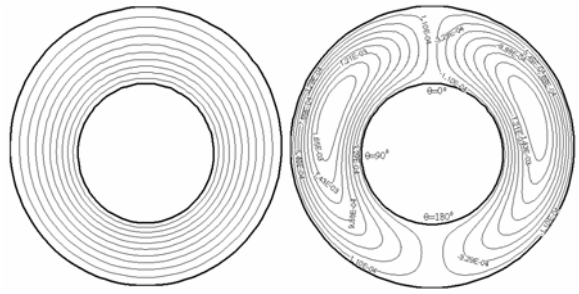

Fig. 13 Isotherms and streamlines for C_2=0.1, α=90° and Gr=10^6

4.4.2.If the relative eccentricity C_2 = 0.2

Figure 14 shows that the isothermal lines are modified significantly, and values of the stream function mentioned in the same figure also increase substantially reflecting a convective transfer, but remains relatively low.

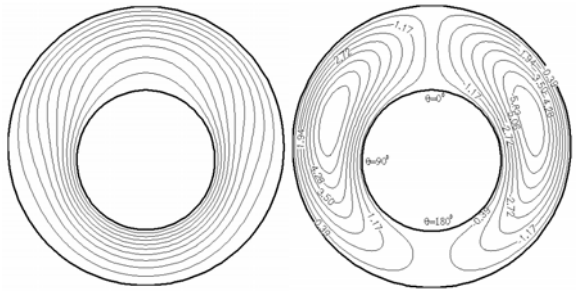

Fig. 14 Isotherms and streamlines for C_2=0.2, α=90° and Gr=10^6

4.4.3. If the relative eccentricity C_2 = 0.4

Figure 15 shows that for large values of Grashof number, the fluid motion is more important in the enlargement area.

The values of the stream function increases with increasing in Grashof number for all geometries considered.

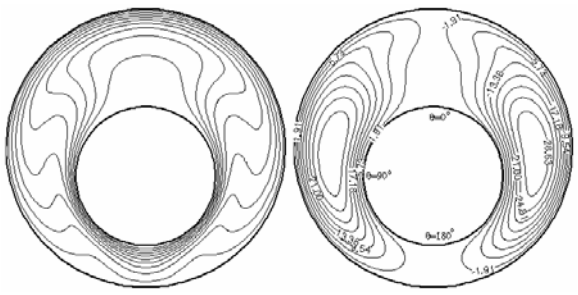

Fig. 15 Isotherms and streamlines for C_2=0.4, α=90° and Gr=10^6

4.5. Influence of the relative eccentricity C_2

Since this study examines the natural convection in an annular space whose geometry varies with the eccentricity, the equivalent thermal conductivity is the parameter most appropriate to compare the heat transfer involved in the various geometries considered. The Nusselt number is proportional to the overall value of the rate of heat transfer consists of the conduction and convection modes, considering that the equivalent thermal conductivity is the ratio of total heat transfer between the inner and outer cylinders, the number of Nusselt is not a good indicator of heat transfer by comparing the different geometries.

The local equivalent thermal conductivity is defined as the ratio of local Nusselt number of a surface in the vicinity of which a fluid is moving in the local Nusselt number that would be determined if the fluid was static. The overall equivalent thermal conductivity is given by the ratio of average Nusselt numbers for either case.

By varying the value of the relative eccentricity of 0.1 to 0.4 for an angle of inclination α = 90 ° and a Grashof number equal to 10^6, we note that the local equivalent thermal conductivity increases with increase in relative eccentricity, reflecting the intensification of natural convection.

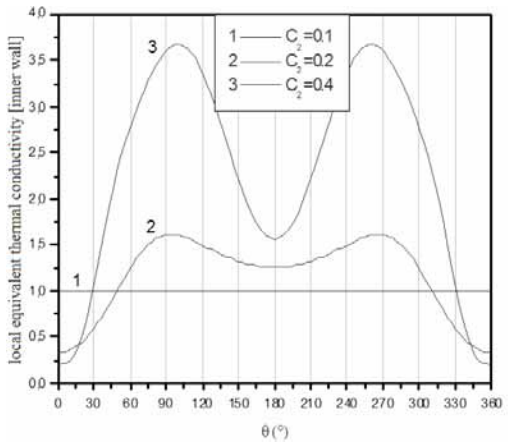

Fig. 16 Variation of the local equivalent thermal conductivity of the inner wall depending

on the θ angle

CONCLUSION

We have established a mathematical model reflecting the transfer of movement within the fluid and heat through the walls of the space annulus. This model is based on the assumption of Boussinesq and the two-dimensionality of the flow. We have developed a calculation code, based on the finite volume method, which determines thermal and dynamic fields in the fluid and the dimensionless local and average Nusselt numbers on the walls of the space annulus, depending on the quantities characterizing the state of the system. The influence of the Grashof number and inclination of the system, on the flow was particularly examined.

The results of numerical simulations have shown that conduction is the regime of heat transfer dominant for

Grashof numbers lower than 5.10^4. For Grashof numbers greater than 5.10^4, the role of convection becomes dominant, and we have seen that the transfers are better when our system has elements of symmetry.

REFERENCES

[1] M.R.H. Nobari, M.T. Mehraba, A numerical study of fluid flow and heat transfer in eccentric curved annuli, Int. J. Thermal. Sciences 49 (2010) 380-396

[2] A. Shklyar, A. Arbel, Accelerated convergence of the numerical simulation of incompressible flow in general curvilinear co-ordinates by discretizations on overset grids, Mathematics and Computers in Simulation 79 (2009) 2476-2489

[3] B. Dukaa, C. Ferrariob, A. Passerinic,, S. Pivac, Non-linear approximations for natural convection in a horizontal annulus, *Int*. J. of Non-Linear Mechanic*s* 42 (2007) 1055–1061

[4] Y. Shi, T.S. Zhao , Z.L. Guo, Finite difference-based lattice Boltzmann simulation of natural convection heat transfer in a horizontal concentric annulus, Computers & Fluids 35 (2006) 1–15

[5] N.A. Roschina , A.V. Uvarov, A.I. Osipov, Natural convection in an annulus between coaxial horizontal cylinders with internal heat generation, Int J. Heat. Mass. Transfer 48 (2005) 4518–4525

[6] S.V. Patankar, Numerical Heat Transfer and fluid flow, McGraw-Hill book company, New-York, 1980

[7] P. Moon, E. Spencer, Field theory Engineers, D. VAN. Nostrand company,LTD, Torronto, 1961

[8] E.F. Nogotov, Applications of Numerical Heat Transfer, McGraw-Hill book company, New-York, 1978

[9] T. H. Kuehn, R. J. Goldstein. Correlating equations for natural convection heat transfer between horizontal circular cylinders, Int. J. Heat Mass Transfer, vol. 19. pp. 1127-1134 (1976)